A New Method for Calculating TE and TM Cutoff Frequencies of Uniform Waveguides with Lunar or Eccentric Annular Cross Section

JAMES R. KUTTLER

Abstract — **Cutoff frequencies are determined for the uniform waveguide with circular outer conductor and eccentric circular inner conductor. The "lunar line" formed by connecting the inner circle to the outer circle is also considered. Both TE and TM modes are treated. The technique used is to combine conformal mapping of the cross section with the powerful method of intermediate problems. This combination of methods has not been applied previously to the calculation of cutoff frequencies. It produces good, rigorous lower bounds for the frequencies. When complementary upper bounds are found by the Ritz method, very small intervals are determined containing the exact frequencies. For the examples considered, the first twenty or so frequencies are bounded very accurately.**

I. Introduction

THE CUTOFF FREQUENCIES of a uniform hollow conducting waveguide are found by solving the Helmholtz equation on the cross section of the waveguide. Many important waveguides have complicated cross sections which cannot be solved by separation of variables. A variety of approximation methods have been used to try to determine the frequencies of such waveguides. It has been observed that a conformal mapping of the cross section can transform the problem to an equivalent anisotropic problem on a geometrically simpler region. It has not been previously observed, however, that this equivalent problem is in a form which is well-suited to the application of the method of intermediate problems.

The method of intermediate problems is a powerful technique which is capable of finding very accurate lower bounds for frequencies. Intermediate methods relate the given problem variationally by an infinite set of constraints to a problem with known solution. When only a finite number of the constraints are used, a solvable problem results which gives the bounds. This method deserves to be more widely known, and it is part of the objective of this paper to popularize this useful procedure. When combined with the more familiar Rayleigh–Ritz method which obtains upper bounds on the frequencies, remarkable accuracy can be achieved with rigorous error bounds, not only for the lowest frequencies but for higher frequencies as well.

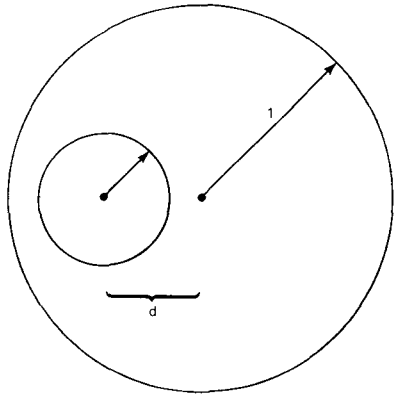

Fig. 1. Eccentric annulus.

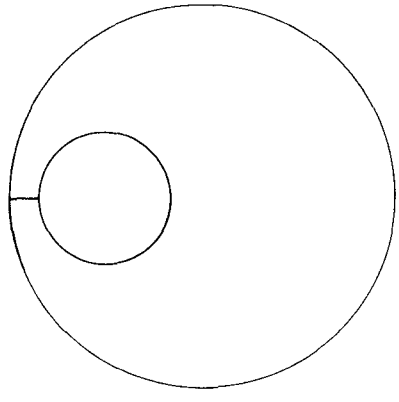

Fig. 2. "Lunar" guide.

This paper exhibits the calculations for a waveguide with circular outer conductor and eccentric circular inner conductor (Fig. 1). When the inner conductor is connected to the outer conductor, the resulting "lunar line" (Fig. 2) is also treated. Frequencies corresponding to both TM and TE modes are given.

The properties of waveguides with these configurations have been a subject of considerable interest. Previous papers on lunar lines include [1], [2], [3] for TE frequencies, [4] for TM frequencies, and [5], [6] for both TM and TE frequen-

Manuscript received December 16, 1983; revised November 14, 1983. This work was supported by the Naval Sea Systems Command, U.S. Department of the Navy, under Contract N00024-83-C-5301.

The author is with the Milton S. Eisenhower Research Center, Applied Physics Laboratory, Johns Hopkins University, Laurel, MD 20707.

0018-9480/84/0400-0348$01.00 ©1984 IEEE

cies. For eccentric annular guides, [7], [8], [9] treated both TM and TE frequencies, while [10]–[14] consider TM frequencies only. Methods employed in these papers include point-matching, finite differences, and truncation of series, sometimes in connection with a conformal mapping. Generally, these papers consider only the lowest few frequencies, and none of them are able to give any estimate of the error in their approximations.

The method presented in this paper, a conformal transformation combined with intermediate methods for lower bounds and Rayleigh–Ritz for upper bounds, essentially solves this important problem once and for all. Tables of numerical results are included which show agreement between the lower and upper bounds to within one or two digits in the third significant figure, even for higher frequencies. Relative dimensions of regions for which frequencies are tabulated were selected to coincide with examples in the literature for purposes of direct comparison. The rigorous bounds on the exact frequencies presented here permits the relative merits of other approximations to be accurately assessed.

The success of the method of intermediate problems for the example of eccentric annular and lunar waveguides hopefully will encourage the employment of this useful tool for other waveguide problems.

II. Conformal Mapping Applied to the Helmholtz Equation

The cutoff frequencies k of a uniform waveguide are determined by solving the Helmholtz equation

$$\frac{\partial^2\Phi}{\partial u^2}+\frac{\partial^2\Phi}{\partial v^2}+k^2\Phi=0 \tag{1}$$

on a region representing the cross section of the waveguide. (We remark that, by analogy, this equation also governs the circular frequencies of vibration of a membrane of the same shape.) For TM modes, the Dirichlet boundary condition

$$\Phi=0 \tag{2}$$

is employed, while for TE modes, the Neumann boundary condition

$$\frac{\partial\Phi}{\partial n}=0 \tag{3}$$

is used. (For a membrane, these correspond, respectively, to fixed or free boundaries.)

The analytic function

$$w=\sinh x_1\coth z/2 \tag{4}$$

maps the rectangle R given by $x_1\leqslant x\leqslant x_2$, $-\pi\leqslant y\leqslant\pi$ in the z-plane onto the slit eccentric annulus between the outer circle having radius l and center at $\cosh x_1$ and the inner circle of radius

$$r=\sinh x_1/\sinh x_2 \tag{5}$$

with center at $\sinh x_1\cosh x_2/\sinh x_2$ (see Fig. 3). If d is the distance between the centers of the circles, the parameters x_1, x_2, r, and d are related by the equations

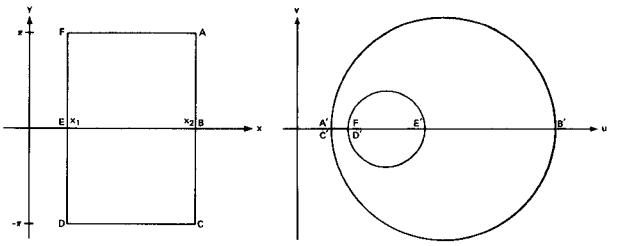

Fig. 3. The map $w=\sinh x_1\coth(z/2)$ transforms a rectangle in the z-plane to the slit eccentric annulus in the w-plane.

$$\cosh x_1=\frac{1-r^2+d^2}{2r} \tag{6}$$

$$\cosh x_2=\frac{1-r^2-d^2}{2rd}. \tag{7}$$

If

$$\phi(x,y)=\Phi(u,v) \tag{8}$$

where $z=x+iy$ and $w=u+iv$ are related by (4), then the Helmholtz equation (1) on the slit annulus is equivalent to the *weighted* Helmholtz equation

$$\frac{\partial^2\phi}{\partial x^2}+\frac{\partial^2\phi}{\partial y^2}+k^2\sigma^2\phi=0 \tag{9}$$

on the rectangle R, where

$$\sigma=\left|\frac{dw}{dz}\right|=(\cosh x-\cos y)^{-1}\sinh x_1. \tag{10}$$

Equation (9) can be thought of as representing a rectangular waveguide composed of an inhomogeneous medium. Dirichlet conditions $\Phi=0$ on a portion of the boundary of the annulus become Dirichlet conditions $\phi=0$ on the corresponding part of the boundary of the rectangle, while Neumann conditions $\partial\Phi/\partial n=0$ are equivalent to Neumann conditions $\partial\phi/\partial n=0$. The function Φ is symmetric or antisymmetric in v if ϕ is symmetric or antisymmetric, respectively, in y.

Consideration of functions ϕ symmetric or antisymmetric in y is not only a convenience, but allows the problem of the complete annulus, as well as the slit annulus (lunar shape), to be considered. The reason is as follows: symmetric functions ϕ satisfying (9) and Dirichlet conditions $\phi=0$ on all sides correspond to symmetric solutions Φ of (8), satisfying $\Phi=0$ on the boundary of the lunar region (including sides of the slit), while antisymmetric functions ϕ satisfying (9) and Dirichlet conditions on all sides correspond to antisymmetric solutions of (8) for *both* the lunar region *and* the eccentric annulus, because antisymmetric functions Φ necessarily vanish on the u-axis. Finally, symmetric solutions of (9) satisfying Dirichlet conditions on $x=x_1$ and $x=x_2$ and *Neumann* conditions $\partial\phi/\partial n=0$ on $y=\pm\pi$ correspond to the symmetric solutions Φ of (8) for the *annulus*, because symmetric functions Φ will satisfy $\partial\Phi/\partial n=0$ on the u-axis. Thus, by considering the various combinations of symmetries and boundary conditions on ϕ, all combinations of symmetries, lunar or annular re-

TABLE I
SYMMETRY AND BOUNDARY CONDITION ON ϕ WITH CORRESPONDING SYMMETRY, MODE TYPE, AND REGION FOR Φ.

Boundary Condition on ϕ		Type of Symmetry	Mode Type of Φ	Type of Region
on $x = x_1$ and $x = x_2$	on $y = \pm n$			
$\phi = 0$	$\phi = 0$	symmetric	TM	lunar
		antisymmetric		lunar or annular
	$\frac{\partial \phi}{\partial n} = 0$	symmetric		annular
$\frac{\partial \phi}{\partial n} = 0$		antisymmetric	TE	lunar
		symmetric		lunar or annular
	$\phi = 0$	antisymmetric		annular

gions, and TM or TE boundary conditions on Φ are obtained. These are summarized in Table I.

III. Method of Obtaining Bounds

By a conformal map, the Helmholtz equation (8) on a complicated region is replaced by the equivalent equation (9) on a simple region at the cost of introducing the weight function σ^2. This latter problem, however, is in a form well-suited for the *method of intermediate problems* [15].

The idea of the intermediate method is to relate the given problem to a problem with known solution (the *base problem*) through an infinite system of constraints. When only a finite number of the constraints are applied, bounds for the desired solution result. By the procedure known as *truncation*, the intermediate problem can be solved by matrix calculation. The method of intermediate problems a powerful technique which deserves to be more widely known. Its application to (9) is illustrated.

Write (9) in the form

$$Au = k^2\sigma^2 u \tag{11}$$

where A is the negative Laplace operator acting on functions in $L_2(R)$, i.e., square integrable functions on the rectangle. Now

$$\max_R \sigma = \sinh x_1$$

so rewrite (11) as

$$Au = k^2\left[\sinh^2 x_1 (I - T^2)\right] u$$

where T is multiplication by

$$\frac{\sqrt{(\cosh x - \cos y)^2 - 1}}{\cosh x - \cos y}.$$

If the positive operator T^2 is dropped, the result is the base problem

$$Au = k^2(\sinh^2 x_1)u \tag{12}$$

which is the just the Helmholtz equation on the rectangle, with the well-known solution found by separation of variables. The frequencies of (12) are lower bounds for the desired frequencies of (11). To improve these bounds, consider an intermediate problem

$$Au = k^2 \sinh^2 x_1 (I - TP_nT)u \tag{13}$$

where P_n is the operator of *orthogonal projection* (in $L_2(R)$) on the span of any convenient set of trial functions $\{p_1, p_2, \cdots, p_n\}$. Then (13) also gives lower bounds for (11), which improve as n is increased.

To reduce the solution of (13) to a matrix calculation, introduce the *truncation* of the operator A. If the frequencies of A are $k_1 \leqslant k_2 \leqslant \cdots$, in order, with associated modes $u_1, u_2, \cdots$, the truncation $A^{(m)}$ of order m agrees with A on $u_1, u_2, \cdots, u_m$ and is multiplication by k_{m+1}^2 on their orthogonal complement. Thus

$$A^{(m)} = AQ_m + k_{m+1}^2(I - Q_m)$$

where Q_m is the orthogonal projection on the span of $\{u_1, \cdots, u_m\}$. Because $A^{(m)}$ is a smaller operator than A, the problem

$$A^{(m)}u = k^2 \sinh^2 x_1 (I - TP_nT)u \tag{14}$$

also has frequencies k, which are lower bounds for the desired frequencies of (11) and increase as both m and n are increased.

Now (14) can be solved as a matrix problem. If

$$u = \sum_{i=1}^{m} a_i u_i + \sum_{j=1}^{n} b_j Tp_j$$

is put into (14), it follows that $m + n$ frequencies of (14) are found from the partitioned relative matrix equation

$$\begin{bmatrix} K^2 & (K^2 - k_{m+1}^2 I)E^t \\ 0 & k_{m+1}^2 B \end{bmatrix} \begin{bmatrix} a \\ b \end{bmatrix} = k^2 \sinh^2 x_1 \begin{bmatrix} I & 0 \\ -E & B - C \end{bmatrix} \begin{bmatrix} a \\ b \end{bmatrix} \tag{15}$$

where K^2 is the diagonal matrix $\operatorname{diag}(k_1^2, k_2^2, \cdots, k_m^2)$ of the first m frequencies of A, and the matrices B, C, and E are given by

$$B_{ij} = \int_R p_i p_j \, dx\, dy \qquad C_{ij} = \int_R Tp_i Tp_j \, dx\, dy$$

$$E_{ij} = \int_R u_i Tp_j \, dx\, dy.$$

The dimensions of B, C, and E are $n \times n$, $n \times n$, and $m \times n$, respectively. Equation (14) also has k_{m+1} as a frequency of infinite multiplicity. In the present problem, it was convenient to choose the trial functions

$$p_j = \sqrt{(\cosh x - \cos y)^2 - 1}\,(\cosh x - \cos y)u_j.$$

Then all integrals required in B, C, and E are elementary.

Complementary upper bounds for the frequencies are obtained from the Rayleigh–Ritz method. Equation (9) is in a very convenient form to apply Rayleigh–Ritz. The Rayleigh quotient for (9) is

$$\frac{\int_R \left[\left(\frac{\partial u}{\partial x}\right)^2 + \left(\frac{\partial u}{\partial y}\right)^2\right] dx\, dy}{\int_R \sigma^2 u^2 \, dx\, dy}. \tag{16}$$

If a linear combination of trial functions

$$u = \sum_{i=1}^{n} a_i \phi_i$$

is used in the Rayleigh quotient (16), the n stationary values of the Rayleigh quotient, with respect to the coefficients a_i, give upper bounds for the squares of the first n frequencies $k_1^2, k_2^2, \cdots, k_n^2$ of (9). For TM modes

$$\phi_i = (\cosh x - \cos y) u_i$$

was used where $u_1, u_2, \cdots, u_n$ are the modes associated with the first n frequencies of the base problem (12). The Rayleigh–Ritz equation then becomes the matrix problem

$$Ma = k^2 (\sinh^2 x_1) a$$

where

$$M_{ij} = \int_R \left[\frac{\partial \phi_i}{\partial x} \frac{\partial \phi_j}{\partial x} + \frac{\partial \phi_i}{\partial y} \frac{\partial \phi_j}{\partial y} \right] dx\, dy$$

and these integrals are elementary. Because the first TE mode is a constant function, this was not a good choice of trial functions for TE modes. Instead

$$\phi_i = u_i$$

was used, making the Rayleigh–Ritz equation

$$K^2 a = k^2 N a$$

where K^2 is again the diagonal matrix $\{k_1^2, \cdots, k_n^2\}$ and

$$N_{ij} = \int_R \sigma^2 u_i u_j\, dx\, dy.$$

These integrals are no longer elementary, so the y integration was done exactly and the x integration approximated by 96-point Gaussian quadratures.

The methods of this paper have been used previously for a circular waveguide with circular ridges [16].

IV. Numerical Results and Comparison with Other Work

The results are always given for an outer circle of unit radius, the radius of the inner circle being denoted r and the distance between the centers of the circles denoted d. To convert these frequencies to those of a similar region with outer circle of radius a, divide these frequencies by a. When comparing the results of other authors, their frequencies were normalized to an outer circle of radius 1. In the tables, the frequencies corresponding to symmetric (s) or antisymmetric (a) modes are identified. Lower bounds are truncated and upper bounds have the last digit rounded up. Note that these are rigorous bounds, and many higher frequencies are obtained.

The information contained in the tables is also summarized graphically in Figs. 4 and 5 for the first two nonzero frequencies. Since the frequencies depend on both r and d, ideally these should be graphed as surfaces in three dimensions. Figs. 4 and 5 are a representation of the projection of data points from these surfaces onto the k-r plane. The range between the upper and lower bounds is represented by rectangles.

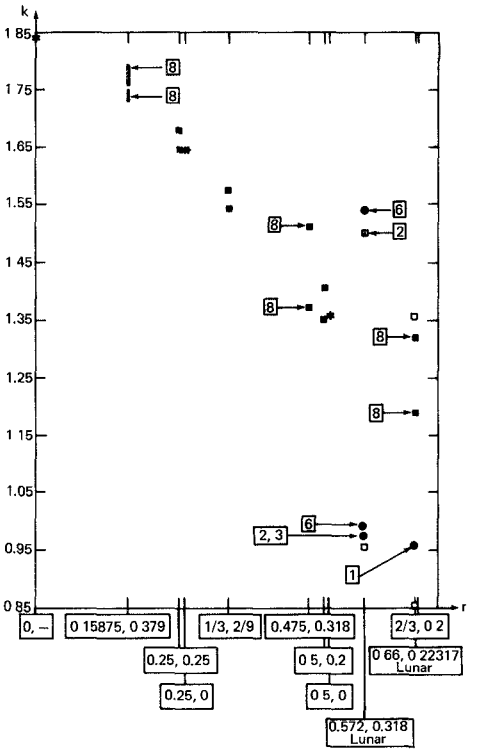

Fig. 4. First two nonzero TE frequencies given in terms of (r, d). Bounds are given by solid rectangles for eccentric annular and open rectangles for lunar guides. Asterisks are exact double frequencies. Results from the literature are also shown as arrows connected to boxes with the number of the reference.

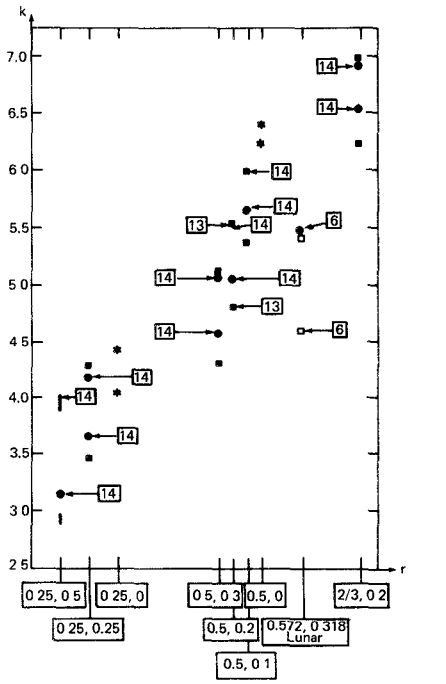

Fig. 5. First two TM frequencies given in terms of (r, d). Bounds are given by solid rectangles for eccentric annular and open rectangles for lunar guides. Asterisks are exact frequencies. Results from the literature are also shown as arrows connected to boxes with the number of the reference.

TABLE II
LOWER AND UPPER BOUNDS FOR FIRST 20 NONZERO TE FREQUENCIES k_j FOR LUNAR GUIDE WITH $r = 0.66$, $d = 0.22317$ CALCULATED BY TRUNCATION WITH $m = n = 60$ AND 64-ORDER RITZ. REFERENCE [1] GIVES $k_2 = 0.96$. (a = ANTISYMMETRIC, s = SYMMETRIC ASSOCIATED MODE.)

J	Lower Bound	Upper Bound	Symmetry
2	0.8521	0.8538	a
3	1.3545	1.3570	s
4	1.8916	1.8952	a
5	2.4619	2.4666	s
6	3.0458	3.0519	a
7	3.6314	3.6392	s
8	4.2138	4.2238	a
9	4.7901	4.8034	s
10	5.359	5.378	a
11	5.916	5.946	s
12	6.035	6.059	s
13	6.465	6.510	a
14	6.843	6.883	a
15	6.984	7.070	s
16	7.502	7.627	a
17	7.62	7.69	s
18	7.97	8.19	s
19	8.35	8.49	a
20	8.45	8.75	a
21	8.63	9.25	s

TABLE III
LOWER AND UPPER BOUNDS FOR FIRST 15 NONZERO TE FREQUENCIES k_j FOR LUNAR GUIDE WITH $r = 0.572$, $d = 0.318$ BY (70,70)-TRUNCATION AND 100-RITZ. NUMBERS IN BRACKETS REFER TO REFERENCES.

J	Lower Bound	Upper Bound	Approximations	Symmetry
2	0 9567	0 9621	0 97547 [2] 0 9745 [3] 0 98975 [6]	a
3	1 4981	1 5026	1 4939 [2] 1 54995 [6]	s
4	2 0448	2 0571	2 11155 [6]	a
5	2 619	2 632	2 74685 [6]	s
6	3 195	3 219		a
7	3 771	3 799		s
8	4 324	4 375		a
9	4 745	4 803		s
10	4 882	4 944		s
11	5 362	5 508		a
12	5 633	5 793		a
13	5 912	6 064		s
14	6 15	6 64		a
15	6 48	6.72		s
16	6 71	7 19		s

TABLE IV
BOUNDS FOR FIRST SEVEN TM FREQUENCIES k_j OF LUNAR GUIDE WITH $r = 0.572$, $d = 0.318$ BY (75,75)-TRUNCATION AND 150-RITZ WITH APPROXIMATIONS.

J	Lower Bound	Upper Bound	[6]	Symmetry
1	4.5962	4.6097	4.60495	s
2	5 4217	5.4433	5.487	a
3	6.2097	6.2383	6.2325	s
4	6.9475	7.0064	6.998	a
5	7.663	7.749		s
6	8.118	8.469		a
7	8 401	8.883		s

Tables II and III give TE frequencies of lunar guides. The guide of Table II has the same relative dimensions as that of [1], where only the lowest frequency was approximated as $k_2 = 0.96$, seen to be high by 12 percent. The guide of Table III was studied in [2] by conformal mapping and series truncation, and in [3] and [5] by finite differences. These results also are shown and most are seen to be slightly high, but this may be accounted for by the fact that these authors considered the line connecting the inner and outer circles to have a positive width. The TM frequencies of this guide are given in Table IV, along with results from [4] and [6] using finite differences.

TABLE V
TM FREQUENCIES k_j FOR ECCENTRIC ANNULAR GUIDES WITH $r = 0.5$, $d = 0, 0.1, 0.2, 0.3$. EXACT FROM [17], BOUNDS BY (70,70)-TRUNCATION AND 140-RITZ. APPROXIMATIONS FROM [13] FOR $d = 0.2$.

	d = 0	d = 0.1			d = 0.2				d = 0.3		
J	Exact	Lower Bound	Upper Bound	Symmetry	Lower Bound	Upper Bound	[13]	Symmetry	Lower Bound	Upper Bound	Symmetry
1	6 2461	5 46911	5 47043	s	4 80953	4.81191	4 811	s	4 3042	4.3118	s
2	6.3932	5.99121	5.99257	a	5.5098	5.5125	5 511	a	5 1179	5 1257	a
3	6 3932	6.47403	6.47547	s	6.1703	6 1735	6 172	s	5.8736	5.8944	s
4	6.8138	6.91953	6.92102	a	6.7964	6 8002		a	6.5994	6.6251	a
5	6 8138	7.30527	7.30683	s	7.3907	7.3957	7 391	s	7.240	7.325	s
6	7.4577	7 71130	7 71299	a	7.9559	7.9619		a	7.876	7.997	a
7	7 4577	7.86823	7.86982	s	8.4894	8.4991		s	8.081	8.316	s
8	8.2667	8.4830	8 4852	a	8.9996	9.0106		a	8.382	8.646	s
9	8.2667	8.4950	8 4972	s	9.2694	9.3488		s	8.829	9 210	a
10	9.1900	9.3542	9 3572	a	9.4528	9.4763		s	8.900	9.276	a
11	9.1900	9.3544	9.3575	s	9.9316	9.9577		a	8.90	9.88	s
12	10 1889	10.3154	10.3199	a	10.000	10.107		a			
13	10.1889	10.3150	10 3199	s	10.207	10.253		s			
14	11.2357	10.709	10.744	s	10.668	10.843		s			
15	11.2357	11.265	11.304	a	10.775	10.852		a			
16	12 3113	11.329	11.340	s	10.821	10.923		s			
17	12.3113	11.331	11.340	a	11.330	11.557		a			
18	12.5469	11 792	11 845	s	11.524	11.777		s			
19	12 6247	12 308	12.365	a	11.568	11 769		a			
20	12.6247	12 365	12 393	s	11.78	12.26		s			
21	12.8555	12 379	12 393	a	12.00	12 74		s			
22	12 8555	12 789	12 865	s	12.27	12.74		a			
23	13.2319	13 265	13 345	a	12.34	12 93		a			
24	13 2319	13 383	13 468	s							
25	13 4030	13 436	13 466	a							
26	13 4030	13 689	13 803	s							
27	13 7423	14.125	14.239	a							
28	13 7423	14 384	14 553	s							

TABLE VI
TM FREQUENCIES FOR ECCENTRIC ANNULAR GUIDES. EXACT FROM [17], BOUNDS BY (70,70)-TRUNCATION AND 140-RITZ.

				r = 0.25						
	r = 2/3, d = 0.2			d = 0	d = 0.25			d = 0 5		
J	Lower Bound	Upper Bound	Symmetry	Exact	Lower Bound	Upper Bound	Symmetry	Lower Bound	Upper Bound	Symmetry
1	6 2379	6.2420	s	4.0977	3.4687	3 4752	s	2.887	2 996	s
2	6.9654	6.9702	a	4 4475	4.2583	4.2660	a	3.858	4.043	a
3	7.6728	7.6787	s	4.4475	4 9110	4.9249	s	4 088	4.827	s
4	8.3631	8 3700	a	5 3199	5.5239	5.5425	a	4.58	5 575	a
5	9 0323	9.0456	s	5.3199	5 893	5.930	s		5.877	s
6	9.6922	9 7071	a	6 4265	6.582	6.641	a		6.323	s
7	10.318	10.356	s	6.4265	6.591	6 723	s		6.992	a
8	10.947	10.992	a	7.5984	6.622	6.767	s		7 208	a
9	11 539	11.616	s	7.5984	7.443	7 723	a		7.735	s
10	12.018	12.174	s	8.3238	7.365	7 739	s		8 166	s
11	12.128	12.229	a	8.5369	7.488	7 735	a		8.355	a
12	12 62	12.84	s	8.5369						
13	12.70	12.93	a							
14	13.15	13.43	a							

Tables V and VI give TM frequencies of eccentric annular guides. In Table V, the inner radius is held fixed at $r = 0.5$, and the offset of the centers d is varied over the values 0, 0.1, 0.2, and 0.3. A concentric annulus ($d = 0$) can be solved exactly. Its TM frequencies k are roots of the equations

$$J_n(k)Y_n(kr) - J_n(kr)Y_n(k) = 0 \qquad (17)$$

where J_n, Y_n are Bessel functions of the first and second kind, and $n = 0, 1, 2, \cdots$. A convenient seven-place table of roots for $n = 0(1)10$ and $r = 0(0.05)0.95$ is [17]. Notice that roots associated with $n = 0$ are single roots, but roots for $n \geqslant 1$ are double since one associated mode has an angular component of $\cos n\theta$, while the other has $\sin n\theta$. From Table V, observe that these double frequencies *bifurcate* or split into distinct frequencies as the inner circle becomes eccentric. The fundamental frequency decreases rather rapidly with increasing eccentricity. Other frequencies decrease less rapidly, while some actually increase for small eccentricities and then decrease. If graphs were drawn of

the frequencies versus eccentricity, some of the curves would appear to cross as indicated by exchanges in relative positions of symmetric and antisymmetric frequencies. Approximations from [13] using truncated series of Bessel functions are also given in Table V, which are in good agreement with the bounds.

Table VI gives bounds for $r = 2/3$, $d = 0.2$, and $r = 0.25$, $d = 0.5$ and 0.25, as well as the exact frequencies for the concentric annulus with $r = 0.25$. Notice that the region with $r = 0.25$, $d = 0.25$ contains the region with $r = 0.5$, $d = 0.2$, which in turn contains the region with $r = 2/3$, $d = 0.2$. It is well known that the TM frequencies are monotone with respect to domain inclusion, and this phenomenon can be observed here.

Graphs are shown of TM frequencies as a function of eccentricity in [8], [9], and [13]. Point matching is used in [8] to give the first five frequencies for $r = 0.25$ and $r = 0.5$; in [9], a perturbation method gives the first frequency for $r = 0.25$; and in [13], the first five to seven frequencies are given for $r = 0.1$, 0.3, and 0.5. These graphs are interesting qualitatively as showing the variation of the frequencies with the offset, but quantitatively are difficult to read with accuracy beyond about 5 percent. Within 5 percent, these graphical results agree with the bounds of the tables, but note that the relative error between the tabulated upper and lower bounds for the lower frequencies is generally $\ll 1$ percent.

The graphical results of our Fig. 4 should be compared with [8, figs. 5–8], and those of our Fig. 5 should be compared with [8, figs. 9 and 10], [9, fig. 4], and [13, fig. 2].

The results obtained in [14] by truncation of Bessel function series do not compare well with the bounds. The approximations reported there are sometimes too low, sometimes too high, and some of the higher frequencies reported are very high (e.g., [14] gives for $r = 2/3$, $d = 0.2$, $k_7 = 11.8719$, whereas $k_7 \leqslant 10.3553$; for $r = 0.5$, $d = 0.2$, $k_9 = 12.3224$, whereas $k_9 \leqslant 9.3488$; for $r = 0.5$, $d = 0.3$, $k_7 = 9.9978$, whereas $k_7 \leqslant 8.316$; for $r = 0.25$, $d = 0.5$, $k_5 = 7.4380$, whereas $k_5 \leqslant 5.877$). Furthermore, [14] incorrectly reports the values of k_1 and k_2 given in [13] for $r = 0.5$, $d = 0.2$.

Tables VII, VIII, and IX report bounds for TE frequencies of various eccentric annuli, as well as exact values for the circle and some concentric annuli. Concentric annuli have frequencies k which are roots of the equations

$$J_n'(k)Y_n'(kr) - J_n'(kr)Y_n'(k) = 0 \qquad (18)$$

where the prime denotes derivative, and $n = 0, 1, 2, \cdots$. These are also tabulated in [17] for $n = 0(1)10$ and $r = 0(0.05)0.95$. It is very important to observe that the first nonzero root for $n = 0$ is *not the lowest frequency*. The lowest nonzero frequency is the double first root for $n = 1$ and the single first root for $n = 0$ gives a higher frequency. Again, all roots for $n \geqslant 1$ are double and bifurcate as the inner circle becomes eccentric.

Tables VII and VIII also given the approximations of [8], where a graph is also given of the lowest four TE

TABLE VII
FIRST 20 NONZERO TE FREQUENCIES k_j FOR ECCENTRIC ANNULAR GUIDE. EXACT FROM [17], BOUNDS FROM (60,60)-TRUNCATION AND 64-RITZ. APPROXIMATIONS FROM [8].

	r = 2/3, d = 0.2				r = 1/2, d = 0.2			r = 1/2, d = 0
j	Lower Bound	Upper Bound	[8]	Symmetry	Lower Bound	Upper Bound	Symmetry	Exact
2	1.19001	1.19176	1.191	a	1.35114	1.35219	a	1.3547
3	1.32027	1.32221	1.322	s	1.40694	1.40793	s	1.3547
4	2.4267	2.4305		a	2.6815	2.6840	a	2.6812
5	2.4408	2.4446		s	2.6837	2.6862	s	2.6812
6	3.6142	3.6211		a	3.9247	3.9298	a	3.9578
7	3.6157	3.6218		s	3.9247	3.9298	s	3.9578
8	4.7804	4.7899		a	4.9937	5.0192	s	5.1752
9	4.7804	4.7901		s	5.1036	5.1138	a	5.1752
10	5.9218	5.9385		s	5.1031	5.1139	s	6.3389
11	5.9231	5.9385		a	5.793	5.834	a	6.3389
12	6.3321	6.3499		s	6.234	6.261	s	6.3932
13	7.027	7.068		s	6.240	6.262	a	6.5649
14	7.035	7.067		a	6.542	6.599	s	6.5649
15	7.111	7.139		a	7.236	7.311	a	7.0626
16	7.867	7.911		s	7.302	7.385	s	7.0626
17	8.075	8.184		s	7.334	7.392	a	7.4622
18	8.093	8.182		a	7.881	7.994	s	7.4622
19	9.060	9.296		s	8.304	8.500	s	7.8401
20	9.089	9.292		a	8.333	8.493	a	7.6401
21	9.251	9.412		s	8.483	8.626	a	8.5586

TABLE VIII
TE FREQUENCIES k_j FOR ECCENTRIC ANNULAR GUIDES. EXACT FROM [17], BOUNDS FROM (60,60)-TRUNCATION AND 64-RITZ. APPROXIMATIONS FROM [8].

	r = 0.475, d = 0.315				r = 0.15875, d = 0.379				r = 0
j	Lower Bound	Upper Bound	[8]	Symmetry	Lower Bound	Upper Bound	[8]	Symmetry	Exact
2	1.3715	1.3741	1.3739	a	1.7330	1.7584	1.7581	a	1.8412
3	1.5132	1.5159	1.5158	s	1.7603	1.7948	1.7946	s	1.8412
4	2.7125	2.7198		a	2.873	2.989		a	3.0542
5	2.7270	2.7345		s	2.871	3.004		s	3.0542
6	3.8978	3.9248		s	3.432	3.775		s	3.8317
7	3.9069	3.9247		a	3.78	4.17		a	4.2012
8	4.342	4.407		s	3.76	4.21		s	4.2012
9	4.977	5.084		s					
10	5.041	5.083		a					
11	5.325	5.427		a					
12	5.919	6.206		s					
13	6.108	6.223		a					
14	6.148	6.387		s					

TABLE IX
TE FREQUENCIES k_j FOR ECCENTRIC ANNULAR GUIDES. EXACT FROM [17], BOUNDS BY (60,60)-TRUNCATION AND 64-RITZ.

	r = 1/3, d = 2/9			r = 0.25, d = 0.25			r = 0.25, d = 0
j	Lower Bound	Upper Bound	Symmetry	Lower Bound	Upper Bound	Symmetry	Exact
2	1.5393	1.5436	a	1.6446	1.6490	a	1.6445
3	1.5766	1.5807	s	1.6768	1.6811	s	1.6445
4	2.8966	2.9067	a	2.9445	2.9684	s	3.0093
5	2.8968	2.9067	s	2.9547	2.9682	a	3.0093
6	4.0944	4.1161	s	3.939	3.988	s	4.1936
7	4.0955	4.1161	a	4.120	4.160	a	4.1936
8	4.2146	4.2356	s	4.105	4.168	s	4.4475
9	5.131	5.167	a	4.978	5.060	a	5.0045
10	5.219	5.270	s	5.111	5.303	s	5.0045
11	5.237	5.279	a	5.175	5.302	a	5.3164
12	5.898	5.954	s	5.602	5.780	s	5.3164
13	6.243	6.396	s	5.89	6.43	s	6.3572
14	6.288	6.392	a	6.08	6.43	a	6.3572
15	6.578	6.664	a	6.31	6.57	a	6.4154
16	6.938	7.071	s	6.27	6.76	s	6.4154

frequencies for $r = 0.5$ as a function of eccentricity (again agreeing, to the limited accuracy of the graph, with the bounds). The numerical results of [8] are consistently near the upper bounds, and perhaps could be shown to always furnish upper bounds to the exact frequencies.

The bounds in Table IX for $r = 1/3$, $d = 2/9$ were intended for comparison with results in [11], where eccentric annuli of these relative dimensions were considered using conformal mapping with point matching. Unfor-

tunately, absolute dimensions are not clearly indicated in [11], and no reasonable normalization of the frequencies reported there makes them correspond to those of the table. Apparently, it was assumed in [11] that the mode without angular dependence furnishes the lowest nonzero frequency, which, as observed above, is not so. The paper [9] may have made this same error ([11] is cited there as a reference). The graph given in [9] for the lowest TE mode for $r = 0.25$ versus eccentricity does not make sense, even for the concentric annulus.

Note that the annulus with $(r, d) = (2/3, 0.2)$ is contained in both $(0.5, 0.2)$ and $(0.475, 0.315)$, which are both contained in $(1/3, 2/9)$, which is contained in both $(0.25, 0.25)$ and $(0.15875, 0.379)$, which are contained in the full circle ($r = 0$). It is interesting to examine the behavior of the frequencies with respect to inclusion. The lower frequencies generally decrease as the inner circle increases, but some of the higher frequencies (e.g., k_8, k_{11}) actually increase at times. Notice that the double frequencies of the full circle stay close to one another, in general. The single frequency corresponding to the $n = 0$ Bessel function tends to migrate up the spectrum with increasing inner-circle size. It is easy to identify because it is associated with a symmetric mode. For $r = 0$, it is k_6; for $r = 1/3$, $d = 2/9$, it is k_8; when $r = 2/3$, $d = 0.2$, it has become k_{12}.

References

[1] A. Y. Hu and A. Ishimaru, "The dominant cutoff wavelength of a lunar line," *IRE Trans. Microwave Theory Tech.*, vol. MTT-9, pp. 552–556, Nov. 1961.

[2] H. H. Meinke, K. P. Lange, and J. F. Ruger, "TE- and TM-waves in waveguides of very general cross section," *Proc. IEEE*, vol. 51, pp. 1436–1443, Nov. 1963.

[3] J. B. Davies and C. A. Muilwyk, "Numerical solution of uniform hollow waveguides with boundaries of arbitrary shape," *Proc. Inst. Elec. Eng.*, vol. 113, pp. 277–284, Feb. 1966.

[4] M. J. Beaubien and A. Wexler, "An accurate finite-difference method for higher-order waveguide modes," *IEEE Trans. Microwave Theory Tech.*, vol. MTT-16, pp. 1007–1017, Dec. 1968.

[5] H. H. Meinke and W. Baier, "Die Eigenschaften von Hohlleitern allgemeineren Querschnitts," *Nachrichtentech. Z.*, vol. 11, pp. 662–670, 1966.

[6] M. J. Beaubien and A. Wexler, "Unequal-arm finite-difference operators in the positive-definite successive over-relaxation (PDSOR) algorithm," *IEEE Trans. Microwave Theory Tech.*, vol. MTT-18, pp. 1132–1149, Dec. 1970.

[7] E. Abaka and W. Baier, "TE and TM modes in transmission lines with circular outer conductor and eccentric circular inner conductor," *Electron. Lett.*, vol. 5, pp. 251–252, 1969.

[8] H. Y. Yee and N. F. Audeh, "Cutoff frequencies of eccentric waveguides," *IEEE Trans. Microwave Theory Tech.*, vol. MTT-14, pp. 487–493, Oct. 1966.

[9] F. E. Eastep, "Estimation of fundamental frequency of doubly-connected membranes," *J. Sound Vibration*, vol. 37, pp. 399–410, 1974.

[10] G. I. Veselov and S. G. Semenov, "Theory of circular waveguide with eccentrically placed metallic conductor," *Radio Eng. Electron. Phys.*, vol. 15, pp. 687–690, 1970.

[11] M. J. Hine, "Eigenvalues for a uniform fluid waveguide with an eccentric-annulus cross-section," *J. Sound Vibration*, vol. 15, pp. 295–305, 1971.

[12] M. J. Hine and F. J. Fahy, "A membrane analogy to an acoustic duct," *J. Sound Vibration*, vol. 37, pp. 399–410, 1974.

[13] K. Nagaya, "Vibration of a membrane having a circular outer boundary and an eccentric circular inner boundary," *J. Sound Vibration*, vol. 50, pp. 545–551, 1977.

[14] W. H. Lin, "Free transverse vibrations of uniform circular plates and membranes with eccentric holes," *J. Sound Vibration*, vol. 81, pp. 425–435, 1982.

[15] D. W. Fox and W. C. Rheinboldt, "Computational methods for determining lower bounds for eigenvalues of operators in Hilbert space," *SIAM Rev.*, vol. 8, pp. 427–462, 1966.

[16] J. R. Kuttler and V. G. Sigillito, "Eigenvalues of the Laplacian in two dimensions," *SIAM Rev.*, to be published.

[17] J. Weil, T. S. Murty, and D. B. Rao, "Zeros of $J_n(\lambda)Y_n(\eta\lambda) - J_n(\eta\lambda)Y_n(\lambda)$ and $J_n'(\lambda)Y_n'(\eta\lambda) - J_n'(\gamma\lambda)Y_n'(\lambda)$," *Math. Comput.*, vol. 22, microfiche supplement, 1968.

James R. Kuttler was born in Burlington, IA, in 1941. He received the B.A. degree in mathematics from Rice University, Houston, TX, in 1962, the M.A. degree in 1964, and the Ph.D. degree in 1967 in applied mathematics from the University of Maryland, College Park, MD.

Since 1967, he has been a Senior Mathematician with the Johns Hopkins University Applied Physics Laboratory, performing basic research and consulting on the numerical solution of partial differential equations. He is a specialist in finite-differences, elliptic eigenvalue problems, *a priori* inequalities, and large matrix systems, with applications to vibrations of structures, waveguides, fluid dynamics, and chemical phase-transition problems.

Dr. Kuttler is a member of the Society of Industrial and Applied Mathematics and the American Mathematical Society.